

# Original Research Article

## Influence of Climatic and Oceanographic Parameters on CO<sub>2</sub> Exchanges at the Air-Sea Interface in the Gulf of Guinea

### ABSTRACT

**Aims:** Analyze the climatic and oceanographic parameters influencing oceanic CO<sub>2</sub>.

**Place and Duration of Study:** Gulf of Guinea, 2010-2018

**Methodology:** Analysis of Monthly Satellite Data from the Gulf of Guinea on Sea Surface Temperature, Sea Surface Salinity, Sea Surface Chlorophyll, Sea Surface Partial Pressure of CO<sub>2</sub>, Sea Surface Wind Speed at 10 meters, Dry Air Molar Fraction (xCO<sub>2</sub>), and Sea Level Pressure. Numerical Data Processing on a One-Degree Spatial Resolution Grid Using Python 3.11 through Bilinear Interpolation

**Results:** Physical parameters (salinity, temperature, wind speed), hydrological parameters (chlorophyll-a and ocean surface partial pressure of CO<sub>2</sub>) are characterized by strong seasonal and spatial variability, modulated by phenomena such as seasonal upwelling and thermal stratification, which directly influence CO<sub>2</sub> fluxes at the air-sea interface, with minor differences between coastal areas and offshore regions.

**Conclusion:** Climatic and oceanographic parameters act synergistically to modulate CO<sub>2</sub> exchanges between the ocean and the atmosphere. Integrating these parameters into climate models will improve the accuracy of global climate change predictions.

**Key words :** Oceanographic parameters, Gulf of Guinea, Python, CO<sub>2</sub>.

### 1. INTRODUCTION

The Gulf of Guinea, located along the west coast of Africa, is a region of significant ecological and economic importance. This portion of the tropical Atlantic Ocean exhibits characteristics that influence climatic and oceanographic factors through complex interactions. Among these factors, air-sea interface interactions play a crucial role in the carbon cycle, particularly in the transfer of carbon dioxide (CO<sub>2</sub>) between the atmosphere and the ocean [1]. Understanding these parameters is therefore essential for assessing the impact of climate change on carbon cycles and, consequently, on global climate [2]. These parameters include sea surface temperature (SST), sea surface salinity (SSS), sea surface chlorophyll-a (Chl-a), sea surface wind speed (U10), as well as sea surface partial pressure of CO<sub>2</sub> (pCO<sub>2sw</sub>). In the lower atmosphere, the dry air mole fraction of CO<sub>2</sub> (xCO<sub>2</sub>) and sea level pressure (SLP) also influence CO<sub>2</sub> exchange behavior at the air-sea interface, impacting the processes of absorption and emission of this greenhouse gas. Studies by [3] and [4] highlight the importance of these

parameters in modeling CO<sub>2</sub> fluxes at the air-sea interface. Sea surface temperature influences CO<sub>2</sub> solubility, while salinity affects seawater alkalinity and buffering capacity [5]. Chlorophyll-a, as an indicator of biological productivity, plays a key role in CO<sub>2</sub> absorption through photosynthesis [6]. Wind speed is a determining factor for CO<sub>2</sub> transfer between the atmosphere and the ocean, as it influences turbulence at the air-sea interface [7]. In the lower atmosphere, the dry air mole fraction of CO<sub>2</sub> (xCO<sub>2</sub>) and sea level pressure (SLP) are key variables modulating the partial pressure gradients necessary for CO<sub>2</sub> fluxes [8]. These atmospheric parameters, combined with oceanographic conditions, determine the net CO<sub>2</sub> exchanges between the ocean and the atmosphere. The objective of this work is to analyze how each parameter influences CO<sub>2</sub> behavior at the air-sea interface in the Gulf of Guinea. This analysis aims to provide a detailed understanding of the interactions between climatic conditions and oceanic processes that modulate the carbon cycle in this region, thus allowing a better grasp of their climatic implications at the regional scale.

### Study Area Presentation

The Gulf of Guinea is a maritime region located along the west coast of Africa (Figure 1). This vast body of water, covering an area of approximately 3146000 km<sup>2</sup>, extends from the southwest of the African continent to the central part of West Africa. It is longitudinally bounded by the meridians of 15° West and 10° East, and latitudinally by the parallels of 10° North and 0° (equator). This region is influenced by seasonal upwellings that occur along the equator and its coasts.

The Gulf of Guinea holds major strategic and economic importance. It is rich in natural resources, particularly hydrocarbons (oil and natural gas), making this region a key hub for the energy industries. Additionally, it is renowned for its marine biodiversity and coastal ecosystems, which include mangroves, estuaries, and coral reefs.

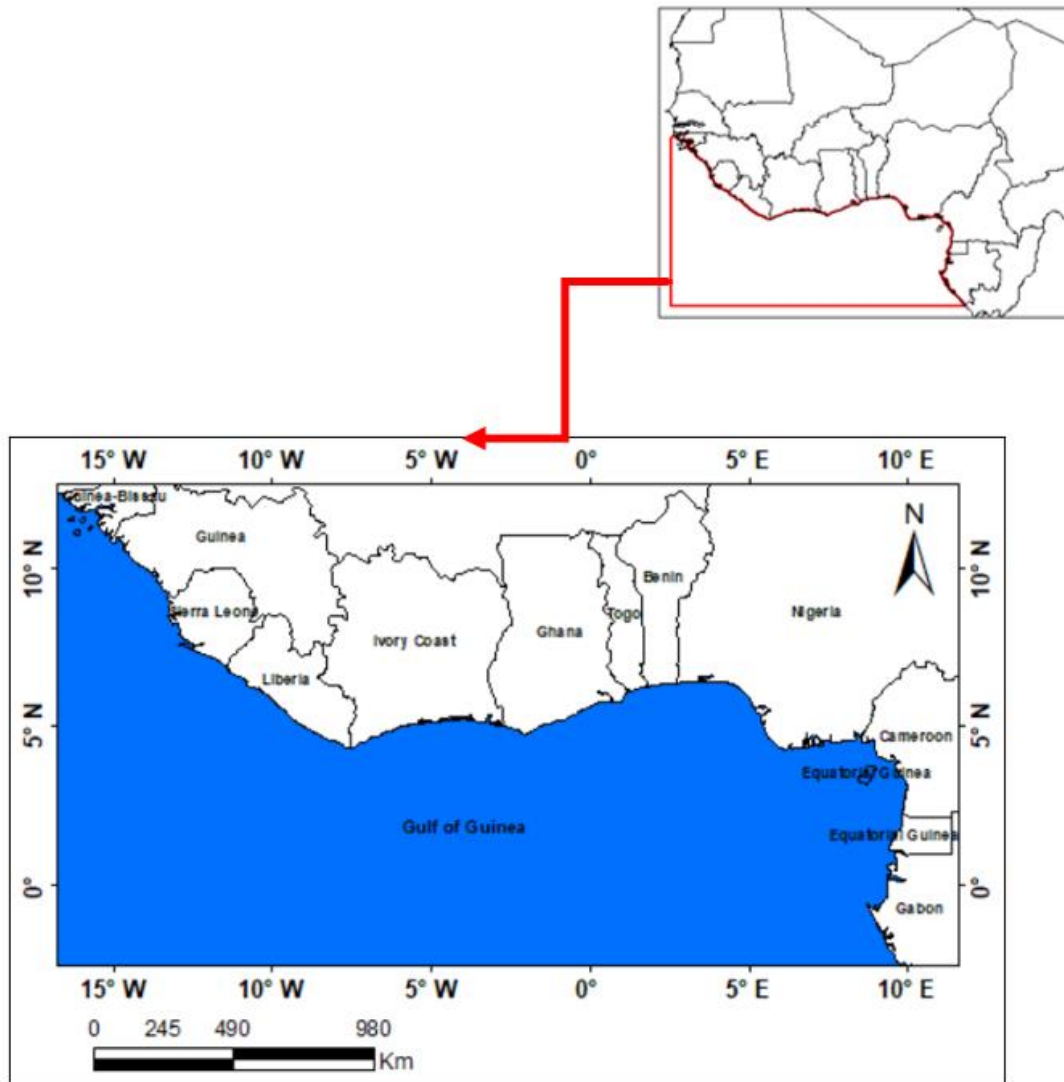


**Fig.1.** Geographical Location of the Gulf of Guinea

## **MATERIAL AND METHODS**

### **2.1 Data collection**

The data used are satellite-based sea surface temperature data acquired from <https://www.ncei.noaa.gov>, sea surface salinity data from <ftp://ftp.ifremer.fr>, chlorophyll-a data from <http://www.oceancolour.org>, and 10-meter wind speed data from [www.remss.com/measurements/ccmp](http://www.remss.com/measurements/ccmp). The data collection period spans from 2010 to 2018. During this period, the data were acquired with a spatial resolution of  $0.25^\circ \times 0.25^\circ$  in longitude and latitude and a temporal resolution of 6 hours (sea surface temperature and wind speed), and 4 days (sea surface salinity). As for the chlorophyll data, they have a spatial resolution of 4 km and a temporal resolution of 8 days, corresponding to a 4 km x 4 km grid for each image pixel. Other types of satellite data were also used, notably from the lower atmosphere, including the dry air mole fraction and air pressure, which are essential for determining gas transfer velocity, solubility, as well as  $p\text{CO}_2\text{w}$  and  $p\text{CO}_2\text{a}$  values. During the same data collection period, these data were obtained from <https://www.esrl.noaa.gov> and provide daily data with a spatial resolution of  $0.25^\circ \times 0.25^\circ$  in longitude and latitude, as well as a temporal resolution of 6 hours.

## **2.2 Methods**

In order to analyze CO<sub>2</sub> exchanges in the Gulf of Guinea, the climatic and oceanographic parameters were processed on a one-degree spatial resolution grid using Python 3.11, ensuring data analysis homogeneity. To achieve this, a custom script written in Python was designed and applied to each dataset, after which the data were regridded using Python libraries such as numpy, xarray, and xesmf. Then, bilinear interpolation was applied to resample the data onto a regular grid with a one-degree resolution. The processed data were saved as NetCDF files, compliant with FluxEngine model standards. Finally, a visual validation was performed using maps generated with matplotlib and cartopy, allowing for the verification that the resampled data maintained geographical consistency.

## **3. RESULTS AND DISCUSSION**

### **3.1 Spatio-temporal Variability of Sea Surface Temperature**

From January to March, temperatures are relatively high, ranging between 28 and 30°C. From April to June, a slight drop in temperatures is observed, particularly along the coast, with values ranging from 27 to 28°C. From July to September, temperatures are lower, oscillating between 25 and 27°C, especially along the southern coast. However, from October to December, they gradually begin to rise, reaching the levels observed at the beginning of the year (28 to 30°C) (Figure 2A).

### **3.2 Spatio-temporal Variability of Sea Surface Salinity**

Figure 2B shows salinity generally ranging from 34 to 37 psu (Practical Salinity Units) in the Gulf of Guinea. Coastal areas exhibit lower salinity, while offshore regions show higher salinity values. Specifically, from January to March, salinity is relatively low (between 34 and 35 psu), especially near the northern part of the equator. From April to June, salinity slightly increases, particularly south of the equator, reaching up to 36 psu. Between July and September, salinity continues to rise, reaching 36.3 psu, especially in August and September. From October to December, salinity decreases again, returning to lower values.

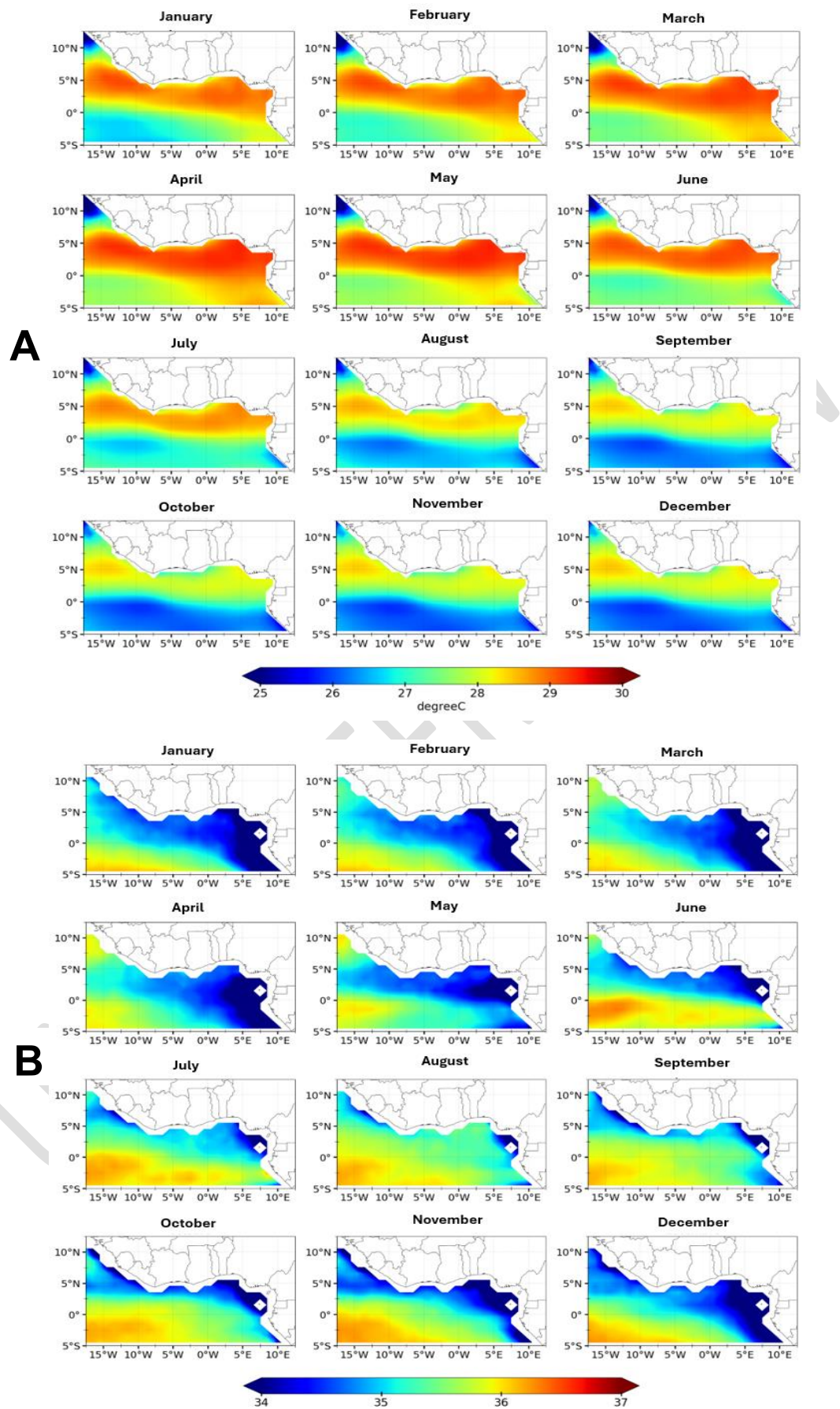


**Fig.2.** Spatial distribution of the monthly average of SST (A) and SSS (B) in the Gulf of Guinea from 2010 to 2018

### **3.3 Spatio-temporal Variability of Sea Surface Chlorophyll-a**

The variability of sea surface Chlorophyll-a shows high chlorophyll concentrations along the coasts of the Gulf of Guinea, ranging between 0.9 and 1 mg.m<sup>-3</sup> during the period from 2010 to 2018. The areas of high chlorophyll concentration are primarily located along the coasts and around the equator, particularly visible from January to March and from July to September, with values around 0.7-1.0 mg.m<sup>-3</sup>. In contrast, the areas of low chlorophyll concentration cover most of the oceanic zone, with a decrease in chlorophyll observed from April to June and from October to December, with near-zero values (Figure 3C).

### **3.4 Spatio-temporal Variability of 10-meter Sea Surface Wind Speed**

Figure 3D shows extreme wind speed values in the study area. Indeed, very high speeds range from 6 to 8 m/s, while the lowest are between 0 and 2 m/s. From January to March, wind speeds are lower, generally between 2 and 4 m/s. Between April and June, a gradual increase in wind speed occurs, reaching 4 to 6 m/s. From July to September, wind speeds continue to increase, peaking in August (up to 8 m/s). However, from October to December, a return to initial values is observed.



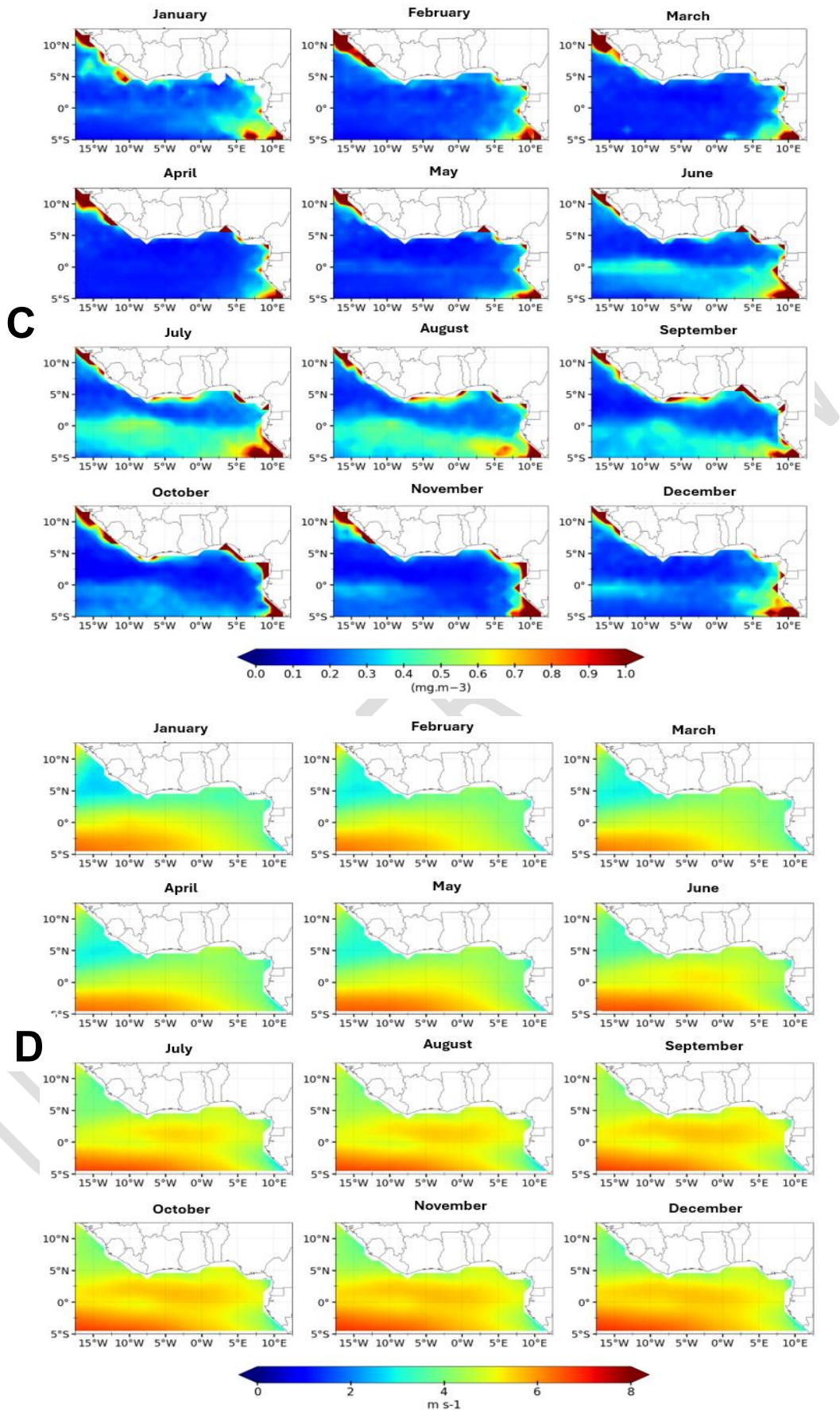


**Fig.3.** Spatial distribution of the monthly average of sea surface chlorophyll (C) and wind speed (D) in the Gulf of Guinea from 2010 to 2018.

### 3.5 Spatio-temporal Variability of Sea Surface Partial Pressure of CO<sub>2</sub>

Figure 4 shows the variation in sea surface partial pressure of CO<sub>2</sub> (PCO<sub>2</sub>sw) in the Gulf of Guinea, ranging from 300 to 650  $\mu\text{atm}$ . From January to March, relatively high concentrations are observed along the coast, ranging between 400 and 500  $\mu\text{atm}$ . From April to June, PCO<sub>2</sub>sw concentrations remain high along the coast, but a downward trend is observable in May. In June, PCO<sub>2</sub>sw increases significantly along the coast, with values reaching up to 550  $\mu\text{atm}$  in certain regions. From July to September, PCO<sub>2</sub>sw concentrations rise even further, particularly in August, peaking at over 600  $\mu\text{atm}$ . In September, concentrations remain high along the coast but tend to decline from October to December. This decline intensifies in November and December, although concentrations of 500  $\mu\text{atm}$  are still present in some areas.

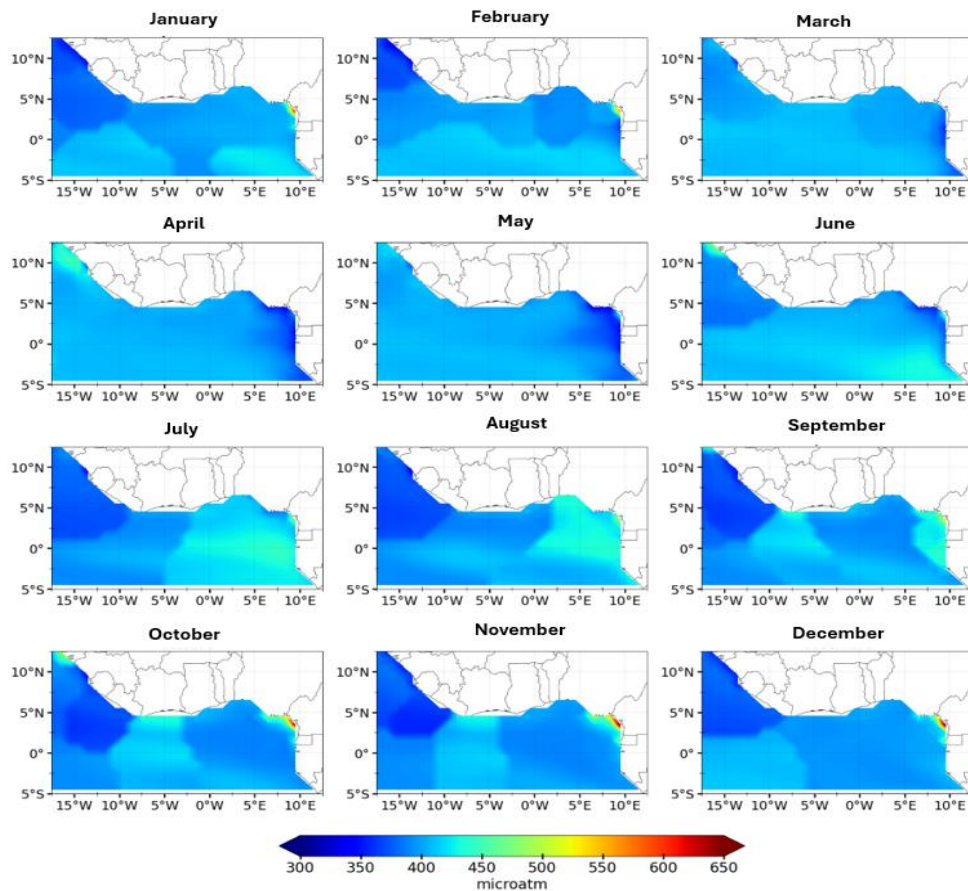


**Fig.4.** Spatial distribution of the monthly average of sea surface partial pressure of CO<sub>2</sub> (PCO<sub>2</sub>sw) in the Gulf of Guinea from 2010 to 2018.

### 3.6. Discussion

The study primarily relied on custom scripts written in Python. These scripts allowed for efficient data rescaling. Indeed, each parameter studied is interconnected and often influences biogeochemical processes at the air-sea interface in various ways. The monthly and seasonal variations in sea surface temperature reveal that during periods of high temperatures (from January to March and from October to December), the ocean's capacity to absorb CO<sub>2</sub> decreases. This suggests weak thermal stratification, leading to increased CO<sub>2</sub> emissions into the atmosphere, as confirmed by the studies of [9] and [10].



These studies address the methods and estimates of anthropogenic CO<sub>2</sub> inventories in the ocean, while considering the effects of temperature on CO<sub>2</sub> solubility. In contrast, during periods of lower temperatures (notably from July to September), the decrease in temperature is attributed to seasonal upwelling, where coastal winds promote the upwelling of colder waters from the depths to the surface, causing a drop in temperatures. [11], [12], and [13] have demonstrated that upwelling brings CO<sub>2</sub>-rich and more acidic waters to the surface, affecting marine ecosystems. Regarding sea surface salinity, it is relatively low, particularly near the northern part of the equator, mainly between January and March, as well as between October and December. This low salinity is attributed to heavy rainfall and freshwater inputs from rivers, such as the Congo River, which reduce salinity, as confirmed by recent studies from [14] and [15]. These authors show that rainfall and riverine inputs have a significant impact on surface salinity in the Gulf of Guinea. Moreover, salinity reaches very high values in August and September, marking the cold season. This increase is due to reduced freshwater inputs as well as increased evaporation. This dynamic is also reinforced by upwelling, which can bring saltier water from the depths to the surface. [15] and [16] confirm that the seasonal variations in salinity in the Gulf of Guinea are strongly influenced by weather conditions and river flows. The monthly and seasonal variations in 10-meter wind speeds in the Gulf of Guinea show that during the major dry season (January-March), weak winds (2-4 m/s), predominantly from the northeast trade winds, bring relatively stable but weak wind conditions. [17] highlighted a correlation between decreased wind speeds and reduced gas fluxes. On the other hand, the strong winds observed during the major cold season, peaking in August (up to 8 m/s), are often linked to the African monsoon, which brings stronger winds and more turbulent conditions, promoting increased CO<sub>2</sub> transfer. The work of [18] and [19] shows how monsoons influence CO<sub>2</sub> fluxes in coastal regions. Chlorophyll-a concentrations, ranging from 0.7 to 1.0 mg/m<sup>3</sup> along the coasts, are corroborated by recent studies. [20] have shown that nutrient inputs, similar to upwelling, increase chlorophyll-a concentrations. Additionally, the decrease in chlorophyll-a concentrations during periods of thermal stratification is confirmed by [21], who demonstrate how seasonal variations influence marine biogeochemical cycles. Sea surface partial pressure of CO<sub>2</sub> (pCO<sub>2</sub>sw) remains slightly elevated along the coasts during the major warm season, then significantly decreases in May. This is explained by lower biological productivity and increased oceanic thermal stratification during this period, as suggested by [3], [22], [23], [24], and [25]. However, during the major cold season, pCO<sub>2</sub>sw is higher from July to September, a period when upwelling currents bring CO<sub>2</sub>-rich waters from the depths, promoting phytoplankton growth and indicating an increase in pCO<sub>2</sub>sw. These results are in agreement with the research of [12], [26], and [27], which showed that intense upwelling events bring CO<sub>2</sub>-rich waters to the surface, thereby increasing pCO<sub>2</sub>sw concentrations.

#### **4. Conclusion**

In conclusion, it is clear that climatic and oceanographic parameters such as sea surface temperature, salinity, chlorophyll-a, wind speed, and partial pressure of CO<sub>2</sub> play a fundamental role in CO<sub>2</sub> exchanges at the air-sea interface in the Gulf of Guinea. The analysis of data from the 2010-2018 period reveals significant spatio-temporal variations, modulated by phenomena such as seasonal upwelling and thermal stratification, which directly influence CO<sub>2</sub> fluxes at the air-sea interface, as higher temperatures reduce the water's ability to absorb CO<sub>2</sub>. Regions with high salinity due to strong

evaporation or low freshwater input can alter CO<sub>2</sub> exchanges, as saltier waters can dissolve less CO<sub>2</sub> than less saline waters, although this effect is relatively small. Areas with stronger winds promote more efficient CO<sub>2</sub> absorption by the ocean. High pCO<sub>2</sub> levels in the water lead to CO<sub>2</sub> degassing into the atmosphere. Thus, these climatic and oceanographic parameters act synergistically to modulate CO<sub>2</sub> exchanges between the ocean and the atmosphere. Integrating these parameters into climate models could improve the accuracy of global climate change predictions.

## References

- [1] Resplandy L., Hogikyan A., Müller J. D., Najjar R. G., Bange H. W., Bianchi D., ... & Regnier P. (2024). A synthesis of global coastal ocean greenhouse gas fluxes. *Global biogeochemical cycles*, 38(1), e2023GB007803.
- [2] Gutiérrez-Loza, L. (2020). Mechanisms controlling air-sea gas exchange in the Baltic Sea. Licentiate dissertation, Uppsala University, 39 pages.
- [3] Takahashi T., Sutherland S. C., Wanninkhof R., Sweeney C., Feely R. A., Chipman D. W., ... & de Baar H. J. (2009). Climatological mean and decadal change in surface ocean pCO<sub>2</sub>, and net sea-air CO<sub>2</sub> flux over the global oceans. *Deep Sea Research Part II: Topical Studies in Oceanography*, 56(8-10), 554-577.
- [4] Wanninkhof R. (2014). Relationship between wind speed and gas exchange over the ocean revisited. *Limnology and Oceanography: Methods*, 12(6), 351-362. <https://doi.org/10.4319/lom.2014.12.351>
- [5] Landschützer P., Gruber N., Bakker D. C., Stemmler I., & Six K. D. (2018). Strengthening seasonal marine CO<sub>2</sub> variations due to increasing atmospheric CO<sub>2</sub>. *Nature Climate Change*, 8(2), 146-150.
- [6] Behrenfeld M. J., Boss E. S., & Halsey K. H. (2021). Phytoplankton community structuring and succession in a competition-neutral resource landscape. *ISME communications*, 1(1), 12
- [7] Watson A. J., Schuster U., Shutler J. D., Holding T., Ashton I. G. C., Landschützer P., et al. (2020). Revised estimates of ocean-atmosphere CO<sub>2</sub> flux are consistent with ocean carbon inventory. *Nature Communications*, 11(1), 1–6. <https://doi.org/10.1038/s41467-020-18203-3>
- [8] Hoegh-Guldberg O., & Bruno J. F. (2010). The impact of climate change on the world's marine ecosystems. *Science*, 328(5985), 1523-1528.
- [9] Sabine C. L., & Tanhua T. (2010). Estimation of anthropogenic CO<sub>2</sub> inventories in the ocean. *Annual review of marine science*, 2(1), 175-198.
- [10] Goodwin P., & Lenton T. M. (2009). Quantifying the feedback between ocean heating and CO<sub>2</sub> solubility as an equivalent carbon emission. *Geophysical research letters*, 36(15).
- [11] Djagoua É. V., Larouche P., Kassi J.B., Affian K., et Saley B. (2011). Variabilité saisonnière et interannuelle de la concentration de la chlorophylle dans la zone côtière du golfe de Guinée à partir des images SeaWiFS. *Revue internationale de télédétection*, 32 (14), 3851-3874.
- [12] Gruber N., Landschützer P., & Lovenduski N. S. (2019). The Variable Southern Ocean Carbon Sink. *Annual Review of Marine Science*, 11, 159-186. DOI : 10.1146/annurevmarine-121916-063407

- [13] Feely, R. A., Doney, S. C., & Cooley, S. R. (2009). Ocean acidification: Present conditions and future changes in a high-CO<sub>2</sub> world. *Oceanography*, 22(4), 36-47. Ocean acidification: Present conditions and future changes in a high-CO<sub>2</sub> world. *Oceanography*, 22(4), 36-47.
- [14] Djakouré S., Penven P., Bourlès B., Koné V., & Veitch J. (2017). Respective roles of the Guinea Current and local winds on the coastal upwelling in the northern Gulf of Guinea. *Journal of Physical Oceanography*, 47(6), 1367-1387. <https://doi.org/10.1175/JPO-D-16-0126.1>
- [15] Da-Allada C. Y., Jouanno J., Gaillard F., Kolodziejczyk N., Maes C., Reul N., & Bourlès B. (2017). Importance of the Equatorial Undercurrent on the sea surface salinity in the eastern equatorial Atlantic in boreal spring. *Journal of Geophysical Research: Oceans*, 122(1), 521–538. <https://doi.org/10.1002/2016JC012342>
- [16] Jouanno J., Marin F., du Penhoat Y., Sheinbaum J., and Molines J. M. (2011). Seasonal heat balance in the upper 100 m of the equatorial Atlantic Ocean, *J. Geophys. Res.*, 116, C09003, doi :10.1029/2010JC006912.
- [17] Lenton A., Matear R. J., & Tilbrook B. (2006). Design of an observational strategy for quantifying the Southern Ocean uptake of CO<sub>2</sub>. *Global Biogeochemical Cycles*, 20(4).
- [18] Koffi K.U. (2011). Distribution des paramètres du carbone et du flux de CO<sub>2</sub> à l'interface air-mer dans l'Est de l'Atlantique tropical (Thèse de doctorat, Université Pierre et Marie Curie-Paris VI).
- [19] Coëtlogon, G.D., Janicot S., & Lazar A. (2010). Variabilité intersaisonnière du couplage océan-atmosphère dans le golfe de Guinée au printemps et en été boréaux. *Revue trimestrielle de la Royal Meteorological Society*, 136 (S1), 426-441.
- [20] Thibodeau P. S., Puggioni G., Strock J., Borkman D. G., & Rynearson T. A. (2024). Long-term declines in chlorophyll a and variable phenology revealed by a 60-year estuarine plankton time series. *Proceedings of the National Academy of Sciences*, 121(21), e2311086121.
- [21] Signorini S. R., Franz B. A., & McClain C. R. (2015). Chlorophyll variability in the oligotrophic gyres : mechanisms, seasonality and trends. *Frontiers in Marine Science*, 2, 1.
- [22] Landschuetzer P., Gruber N., Bakker D.C. (2016). Decadal variations and trends of the global ocean carbon sink. *Global Biogeochemical Cycles* 30(10) :1396–1417.
- [23] Bourgeois T., Orr J. C., Resplandy L., Terhaar J., Ethé C., Gehlen M., & Bopp L. (2016). Coastal-ocean uptake of anthropogenic carbon. *Biogeosciences*, 13(14), 4167-4185.
- [24] Henson S. A., Beaulieu C., & Lampitt R. (2016). Observing climate change trends in ocean biogeochemistry: when and where. *Global change biology*, 22(4), 1561-1571.
- [25] DeVries, T. (2022). The Ocean Carbon Cycle. *Annual Review of Environment and Resources*, 47, 317-341. <https://doi.org/10.1146/annurev-environ-120920-111307>
- [26] Feely R.A., Sabine C.L., Lee K., Berelson W., Kleypas J., Fabry V.J., and Millero F.J. (2004). Impact of anthropogenic CO<sub>2</sub> on the CaCO<sub>3</sub> system in the oceans. *Science* 305(5682):362–366, doi:10.1126/science.1097329. NOAA, 1959
- [27] Wanninkhof, R. (1992). Relationship between wind speed and gas exchange over the ocean. *Journal of Geophysical Research: Oceans*, 97(C5), 7373-7382.